Growth of cubic phase gallium nitride by modified molecular-beam epitaxy

M. J. Paisley, Z. Sitar, J. B. Posthill,[a] and R. F. Davis
Department of Materials Science and Engineering, North Carolina State University, Raleigh, North Carolina 27695-7907

(Received 22 August 1988; accepted 14 November 1988)

Gallium nitride is a compound semiconductor with a wide direct band gap (3.45 eV) and a large saturated electron drift velocity. Nearly all single-crystal thin films grown to date have been wurtzite (hexagonal) structure. Cubic GaN has the potential for higher saturated electron drift velocity and somewhat lower band gap. These properties could increase its applicability for high-frequency devices (such as impact ionization avalanche transit time diodes) as well as short-wavelength light emitting diodes and semiconductor lasers. This paper reports the growth of cubic phase single-crystal thin-film GaN using a modified molecular-beam epitaxy technique. A standard effusion cell was used for gallium, but to activate nitrogen gas prior to deposition, a microwave glow discharge was used. Auger electron spectroscopy showed a nominally stoichiometric GaN film. Transmission electron microscopy with selected area diffraction indicated the crystal structure to be zinc blende.

I. INTRODUCTION

Development and commercialization of light emitting diodes (LED's) and semiconductor lasers in the 1970's generated much interest in the wide-band-gap semiconductor GaN. Since it has a band gap of 3.45 eV (near-UV region) at room temperature, and makes a continuous range of solid solutions with AlN (6.28 eV) and InN (1.95 eV), it is a promising material for UV as well as visible radiation. Gallium nitride also possesses two unique properties required in a semiconductor material to be used in fabricating transit-time-limited [impact ionization avalanche transit time (IMPATT), etc.] microwave power amplifiers. It is predicted to have a large saturated electron drift velocity,[1] which results in short transit times and thus allows the fabrication of high-frequency devices. The other important property is the band gap, which is more than twice that of GaAs and three times that of Si. Since pair-production thresholds scale with the band gap, then a GaN transit-time-limited device in reverse bias at high field would be able to operate at higher voltages. In power amplifiers, the power scales as the square of the voltage, thus GaN would have a significant advantage over Si or GaAs.

Cubic GaN is expected to have even higher saturated electron drift velocity since the lattice is isotropic (lower phonon scattering), further improving the comparison of GaN to Si and GaAs. Using SiC as an analog, it is possible that the cubic phase of GaN would have a lower band gap, though calculations by Pankove and Bloom[2] indicate a band gap nearly the same as the hexagonal phase.

II. EXPERIMENTAL PROCEDURES

A. Growth apparatus

The growth system was a commercial Perkin–Elmer 430 molecular-beam epitaxy (MBE) system modified as described below. It consisted of three major sections: a load lock (base pressure $\approx 5\times10^{-8}$ Torr), a transfer tube (base pressure $\approx 1\times10^{-10}$ Torr) which was used to degas the substrates, and the growth chamber (base pressure $\approx 5\times10^{-11}$ Torr). The growth chamber was equipped with four standard 20-cm^3 effusion cells that contained BN crucibles which were resistively heated with Ta wire heaters. The only cell used during these growth studies was the gallium cell which was charged with 47 g of 99.999 99% pure gallium.

B. Gas source design

One modification was utilization of a microwave glow-discharge plasma to dissociate/activate the N containing gas. The power supply was matched with a 2.45-GHz microwave cavity[3] as the literature indicated that those higher frequencies were more suited to the dissociation of nitrogen.[4,5] A schematic diagram of the microwave glow discharge chamber is shown in Fig. 1. This source was attached in place of a more traditional effusion (or cracker) cell for the group-V element. The nitrogen gas was taken from the boil-off of a 160-l liquid-nitrogen Dewar and purified by a hot copper gettering furnace, and subsequently regulated to the source by a variable leak valve.

C. Substrate growth

Initial growth studies were conducted on in-house produced (100)-oriented β-SiC on Si substrates. (This material has the zinc-blende structure.) A detailed description of the substrate preparation is in an earlier paper.[6] Immediately prior to loading into the system, a protective thermally grown oxide layer was removed in a 49% HF etch.

After outgassing, the samples were introduced into the growth chamber and examined using the *in situ* reflection

FIG. 1. Schematic diagram of the glass nitrogen glow discharge source. The microwave applicator is not shown. Nitrogen gas entered at right from a variable leak valve, passed through the microwave discharge in the middle, and finally entered the MBE chamber on the left. The source was mounted on a 2.75 in. metal seal flange.

 0734-2101/89/030701-05$01.00

TABLE I. Conditions used in GaN growth.

Nitrogen pressure	5×10^{-6}–5×10^{-5} Torr
Microwave power	2–100 W
Gallium temperature	800–950 °C
Substrate temperature	500–700 °C
Growth time	120–450 min
Deposited film thickness	500–1700 Å

high-energy electron diffraction (RHEED) system using a 10-kV beam. The resulting RHEED pattern on the β-SiC substrate showed Kikuchi lines indicative of the good crystalline quality of the substrate.

In preparation for growth, the substrate was constantly exposed to a nitrogen flux (analogous to the operation of arsenic sources in the MBE growth of GaAs). Once conditions had stabilized, the Ga cell shutter was opened and growth began. Above in Table I is shown the range of conditions used during growth.

After the growth was complete, the gallium cell and the substrate were cooled down while the nitrogen source again remained active. The nitrogen source was turned off and the growth chamber was returned to UHV conditions once the substrate temperature was below 400 °C. The sample was then evaluated with RHEED again, to determine crystal structure and to get an initial estimate of film quality.

III. THIN-FILM ANALYSIS

A. Chemistry and morphology

Scanning Auger microscopy (JEOL JAMP-30) was performed on the sample to determine the presence of impurities and nominal composition of the GaN layer. Figure 2 is an Auger spectra taken from the untreated growth surface. The oxygen and carbon peaks are most likely due to surface oxidation and contamination upon exposure to the atmosphere. No other contaminants are observed to the resolution of the instrument (typically $\approx$0.1 at. %).

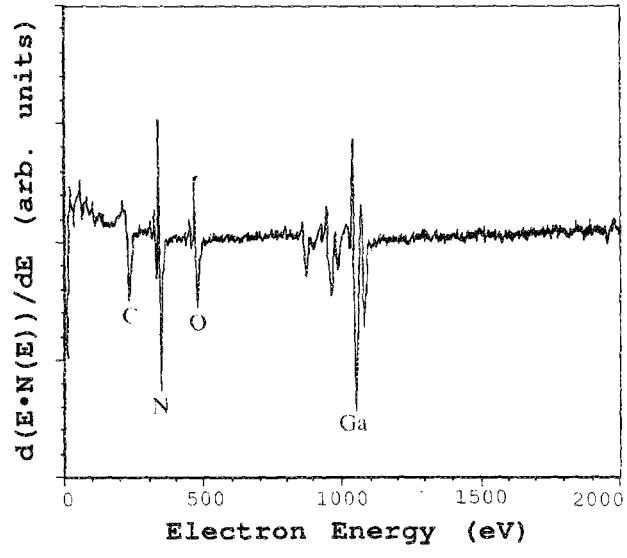

FIG. 2. Auger spectra taken from the untreated GaN surface. Only oxygen and carbon contamination was detected.

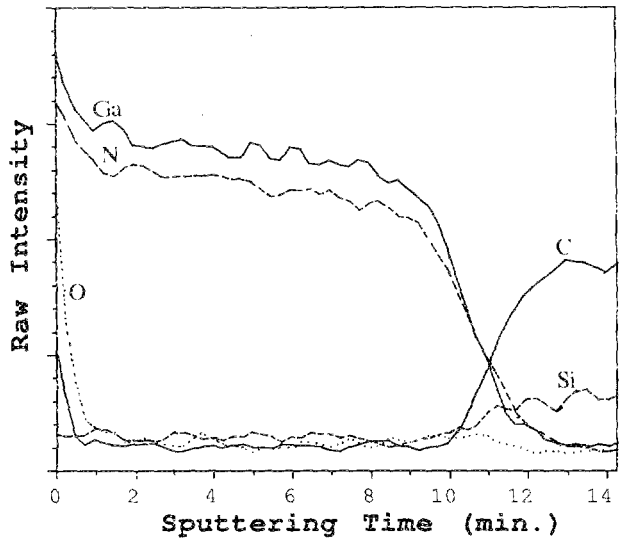

FIG. 3. Auger depth profile of GaN on β-SiC (100). Oxygen and carbon contamination was detected only at the surface. Premature rise in Si and C peaks are likely due to sputtering effects (see the text).

Next a depth profile was performed and is shown in Fig. 3. The depth profile shows that indeed the oxygen and carbon contamination was only on the surface. The apparent depth of the carbon signal into the grown film from the substrate was postulated as being due to a sputtering effect. The sputtering process would open holes in the film down to the substrate allowing the carbon signal to be detected sooner than expected. This is due to roughness in the film surface produced by the sputtering action. The silicon signal indicates a similar behavior albeit to a lesser extent.

The apparent low nitrogen content of the film is due in part to the relative elemental sensitivity factors which when applied, show the N:Ga ratio to be nearly one. Another factor may possibly be a result of the sputtering action of the 3-kV Ar^+ ions. This effect has been seen in InN (by Foley and Lyngdal[7]) which as mentioned in Sec. I, is very similar to GaN. Foley and Lyngdal further observed that the use of Xe^+ ions for sputtering and x-ray photoemission spectroscopy (XPS) minimized the sample decomposition effects better than Ar^+ and Auger electron spectrocopy (AES).

Scanning electron microscopy (Hitachi S-530) was then

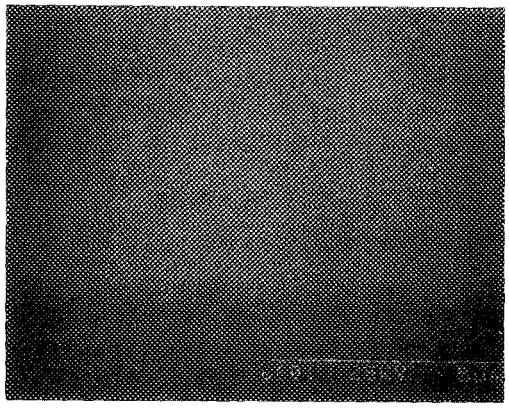

FIG. 4. Scanning electron micrograph of top surface of GaN film.

performed to evaluate the surface morphology of the GaN thin films. As shown in Fig. 4, the surface of the GaN films are, in general, smooth and free of large morphological defects. The defects that were observed were also seen in the β-SiC substrates, and are assumed to have been just reproduced by the growth surface.

B. Structural analysis

Reflection high-energy electron diffraction was performed (as mentioned above) on the β-SiC substrates before, during, and after growth of the GaN layer. Figure 5(a) shows the quality (note Kikuchi lines) of the beginning β-SiC substrate. The initial streaks, which are due to a flat substrate surface, disappeared as growth islands developed [Fig. 5(b)]. Twin spots appeared [Fig. 5(c)] at the $\frac{1}{3}$ distance and then disappeared as initial growth was heavily faulted but then improved [Figs. 5(d) and 5(e)]. Streaks reappeared as the growth islands[5] coalesced and the surface smoothed [Figs. 5(e) and 5(f)].

Transmission electron microscopy (TEM) was utilized (Hitachi H-800) to further assess the microstructure of the GaN epitaxial films. Cross-section TEM (XTEM) speci-

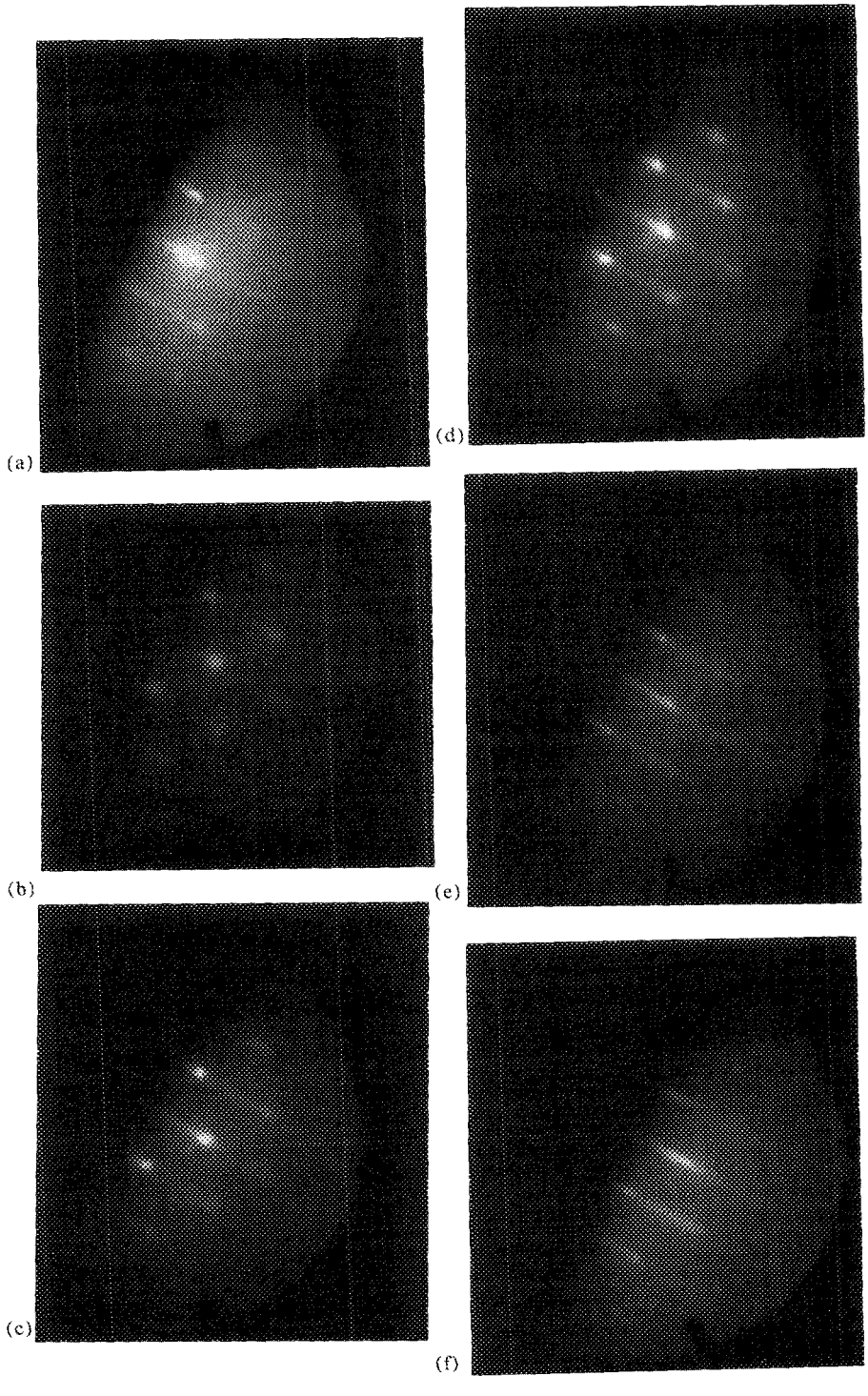

FIG. 5. Time sequence of [110] RHEED photographs at different stages during the growth of a GaN film on a β-SiC(100) substrate: (a) 0 min (before growth was begun), (b) 10 min, (c) 80 min, (d) 130 min, (e) 250 min, and (f) 480 min (after growth).

mens were prepared using standard techniques.[8] Backthinned plan-view TEM specimens were also prepared. All selected area electron diffraction (SAD) patterns taken were fully consistent with the GaN film having a face-centered-cubic Bravais lattice (Fig. 6). In particular, it should be noted that the observation of the [100] SAD pattern [Fig. 6(a)] containing fourfold symmetry could not result from the wurtzite (hexagonal) form of GaN. Also, the 020-type vs 220-type spot intensities indicated that the cubic GaN was ordered in the zinc-blende structure. Furthermore, the crystallographic orientation relationship between the GaN and the β-SiC was found to be epitaxial. The GaN diffraction vectors were measured to be $\cong 4\%$ shorter than the β-SiC reflections; implying that the cubic GaN lattice parameter is roughly 4% larger than the SiC [i.e., a_0 – (β-SiC) ≈ 4.36 Å, hence, a_0 – (GaN) ≈ 4.54 Å]. This value compares well with the calculated value of 4.49 Å, as well as the value reported by Pankove[9] of 4.51 Å for unpublished research, and 4.52–5 Å reported by Mizuta *et al.*[10] for their films grown on GaAs.

Complementary bright-field and dark-field micrographs have also been taken from the cross-section samples. Figure 7 shows that the defect density in the GaN epitaxial film decreased as the distance from the GaN/SiC heteroepitaxial interface increased. Note that the defect density across the film thickness correlates very well with the time sequence of RHEED photographs in Fig. 5. The defects consist of threading dislocations and planar defects.

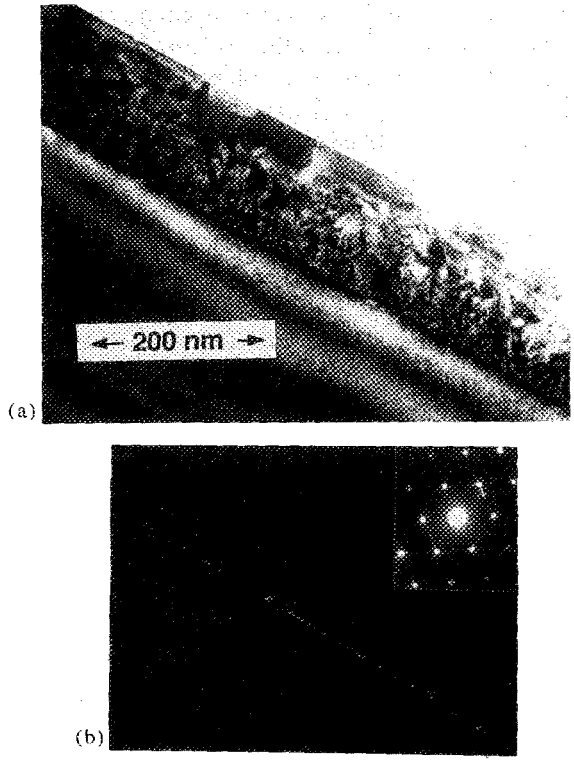

FIG. 7. XTEM micrographs from the GaN/β-SiC structure: (a) bright-field and (b) dark-field micrographs using a 111-type twin reflection. The SAD pattern inset is included and shows the reflection used to form the image.

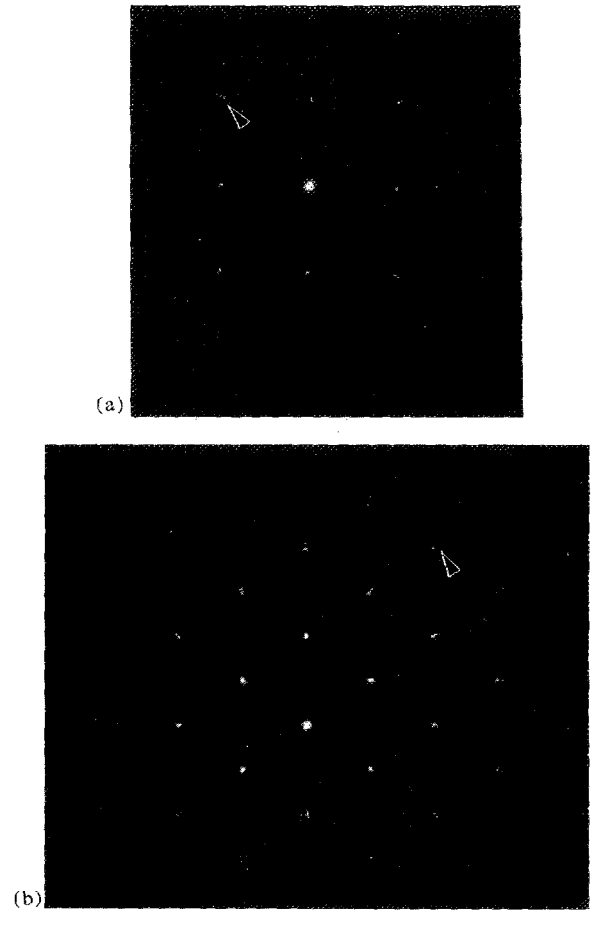

FIG. 6. SAD patterns from GaN/β-SiC(100) heteroepitaxial structure (plan view): (a) [100] pattern, the fourfold symmetry is indicative of a cubic Bravais lattice, (b) [110] pattern obtained after a 45° tilt about [001]. The spot splitting observed at the higher-order reflections (arrows) is due to the superposition of cubic GaN and β-SiC patterns.

The dark-field image was obtained by utilizing a 111-type twin reflection, and hence, many of the planar defects are found to be microtwins. The majority of microtwins emanate from the heteroepitaxial interface but do not extend to the wafer free-surface. Most microtwins are seen to terminate within a distance of 25 nm. This type of microtwin morphology has also been observed in several other heteroepitaxial systems (e.g., Si-on-sapphire[11] and GaAs-on-Si[12]).

High-resolution transmission electron microscopy (HRTEM) was also performed (JEOL 200CX) on these samples (Fig. 8). Several planar defects that lie on {111}-type planes are well resolved and appear to consist of both microtwins and stacking faults. Due to the $\approx 4\%$ lattice mismatch, a regular array of misfit dislocations was expected to be observed at the GaN/SiC interface. This was not found; instead there appeared to be a very thin amorphous interlayer between the two compounds. There were very few regions that displayed perfect crystal/crystal contact between the GaN and the β-SiC. The chemistry of this amorphous interlayer is not known at this time; however, a thin native oxide appears to be the most likely possibility.

Thin, amorphous interlayers have been observed previously at heteroepitaxial interfaces and have sometimes been attributed to a TEM specimen artifact. Both Ar ion milling for TEM specimen thinning[13] and oxidation of the

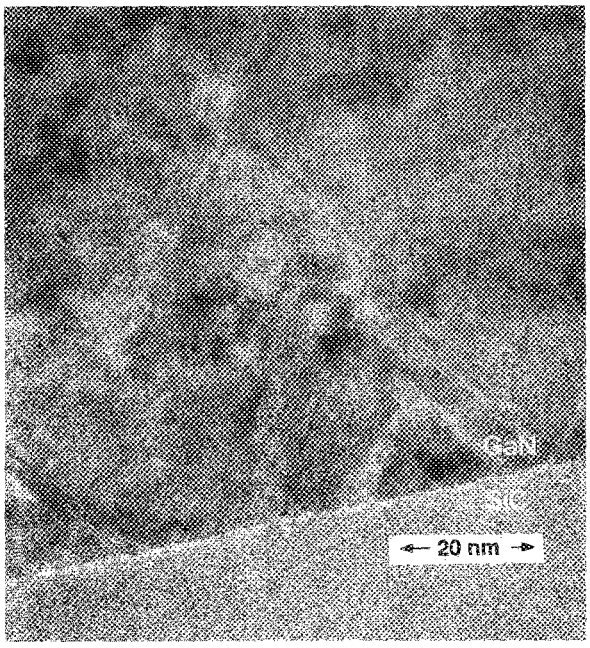

FIG. 8. HRTEM micrograph of the GaN/β-SiC interface in [011] orientation (200 kV, C_s = 1.2 mm). Relatively little area shows continuous lattice fringes across the interface (see the text). Nevertheless, an epitaxial orientation relationship has been maintained.

interface region due to diffusion of oxygen perpendicular to the interface in the thin section[14] have been cited as causes for amorphous interlayer formation in other heteroepitaxial systems. We recognize that some portion of our amorphous interlayer may be due to an artifact, particularly as we observe an increase in the interlayer thickness in the thinnest regions of the TEM specimen. Nevertheless, the fact that the interlayer is still observed in appreciably thicker regions of the TEM specimen leads us to believe that it is not entirely an artifact.

Furthermore, preliminary studies via low-energy electron diffraction (LEED) of the β-SiC substrates indicate the presence of a thin remaining native oxide comparable to that observed by Dayan.[15] It is believed that the presence of this thin oxide has interfered with the initial stages of GaN epitaxy, thereby leading to the extensive microtwin and stacking fault formation. Improved substrate preparation prior to the initiation of growth should enable a reduced microtwin and stacking fault density to be achieved.

The authors also believe that substantial improvements in the growth of GaN can be achieved using atomic layer epitaxy (ALE).[16] This process has resulted in improved characteristics of several materials using either MBE or metalorganic chemical vapor deposition (MOCVD) based systems.[17]

IV. SUMMARY

Thin films of single-crystal zinc-blende GaN were grown on β-SiC(100) substrates over a range of deposition conditions in a modified MBE system using nitrogen flowing through a microwave glow discharge. Electron diffraction clearly showed fourfold symmetry characteristic of the cubic structure as well as spot intensities which indicated an ordered zinc-blende structure. The lattice parameter was measured to be 4.54 Å which was consistent with calculations and values reported in the literature. In addition, XTEM revealed that the film contained threading dislocations and microtwins near the interface, but the defect density dropped rapidly after 25 nm of growth. This profile of defects was also observed by RHEED during growth. HRTEM established that there was epitaxy between the β-SiC substrate and the GaN despite the presence of an interlayer which was a likely cause for the high defect density near the interface. Auger analysis showed that the film was nominally stoichiometric and relatively free from contaminants. The scanning electron micrographs revealed that the top surface was smooth and free from growth-induced defects.

ACKNOWLEDGMENTS

The authors wish to express their appreciation to Mr. Max Yoder (ONR) for his many helpful discussions and worthwhile suggestions. Thanks are also extended to Mr. Brad Williams for his help and suggestions in TEM sample preparation. This work was sponsored by the SDIO/IST and managed by ONR under Contract No. N00014-86-K-0686.

[a] Present address: Research Triangle Institute, Research Triangle Park, NC 27709-2194.

[1] K. Das and D. K. Ferry, Solid-State Electron. **19**, 851 (1976).
[2] J. I. Pankove and S. Bloom, RCA Rev. **36**, 163 (1975).
[3] B. McCarroll, Rev. Sci. Instrum. **41**, 279 (1970); F. C. Fehsenfeld, K. M. Evenson, and H. P. Broida, *ibid.* **36**, 294 (1965).
[4] M. R. Werheimer and M. Moisan, J. Vac. Sci. Technol. A **3**, 2643 (1985).
[5] J. H. Kolts and D. W. Setser, in *Reactive Intermediates in the Gas Phase: Generation and Monitoring*, edited by D. W. Setzer (Academic, New York, 1979).
[6] M. J. Paisley, Z. Sitar, C. H. Carter, Jr., and R. F. Davis, Proc. SPIE **8**, 877 (1988).
[7] C. P. Foley and J. Lyngdal, J. Vac. Sci. Technol. A **5**, 1708 (1987).
[8] J. C. Bravman and R. Sinclair, J. Electron Microsc. Technol. **1**, 53 (1984).
[9] J. I. Pankove, J. Lumin. **7**, 114 (1973).
[10] M. Mizuta, S. Fujieda, Y. Matsumoto, and T. Kawamura, Jpn. J. Appl. Phys. **25**, 1945 (1986).
[11] M. E. Twigg and E. D. Richmond, J. Appl. Phys. **64**, 3037 (1988).
[12] J. B. Posthill, J. C. L. Tarn, T. P. Humphreys, K. Das, J. J. Wortman, and N. R. Parikh, in *Proceedings of the 46th Annual Meeting of the Electron Microscopy Society of America*, edited by G. W. Bailey (San Francisco, San Francisco, 1988), p. 896.
[13] C. H. Carter, Jr., R. F. Davis, and S. R. Nutt, J. Mater. Res. **1**, 811 (1986).
[14] F. K. LeGoues, M. Liehr, M. Renier, and W. Krakow, Philos. Mag. B **57**, 179 (1988).
[15] M. Dayan, J. Vac. Sci. Technol. A **3**, 361 (1985); **4**, 38 (1986).
[16] T. Suntola and J. Antson, U.S. Patent No. 4 058 430 (15 November 1977).
[17] C. H. L. Goodman and M. V. Pessa, J. Appl. Phys. **60**, R65 (1986).